Non-exponential behaviour of pp $d\sigma/dt$ a(p)review

T. Csörgő

Wigner Research Center for Physics, Budapest, Hungary
EKE GYKRC, Gyöngyös, Hungary

Introduction and motivation
Results before LHC
TOTEM results
Interpretations
Results and cross-checks
Outlook
Summary

Theoretically

Using M.M. Block, Phys.Rept. 436 (2006) 71-215

$$f_{\rm c.m.}(s,t) = \frac{1}{k}\sum_{\ell=0}^{\infty}(2\ell+1)P_\ell(\cos\theta)a_\ell(k),$$

$$a_\ell(k) = \frac{e^{2i\delta_\ell}-1}{2i},$$

$$a(b,s) = \frac{e^{2i\delta(b,s)}-1}{2i},$$

$$\begin{aligned} f_{\rm c.m.}(s,t) &= 2k\int_0^\infty b\,db J_0(qb)a(b,s) \\ &= \frac{k}{\pi}\int a(b,s)\,e^{i\vec{q}\cdot\vec{b}}\,d^2\vec{b}, \end{aligned}$$

$$\frac{d\sigma_{\rm el}}{dt} = \frac{\pi}{k^2}|f_{\rm c.m.}|^2 = 4\pi\left|\int a(b,s)J_0(qb)b\,db\right|^2.$$

$$\begin{aligned} \sigma_{\rm el} &= \frac{\pi}{k^2}\int|f_{\rm c.m.}|^2\,dt = \frac{1}{k^2}\int|f_{\rm c.m.}|^2\,d^2\vec{q} \\ &= 4\int|a(b,s)|^2\,d^2\vec{b}. \end{aligned}$$

$$\sigma_{\rm tot} = \frac{4\pi}{k}{\rm Im}\,f_{\rm c.m.}(s,0) = 4\int{\rm Im}\,a(b,s)\,d^2\vec{b}.$$

$$\sigma_{\rm tot} = 2\int{\rm Im}\left[i(1-e^{2i\delta(b,s)})\right]\,d^2\vec{b}.$$

Gray Disc vs Gray Gaussian

For a Gray Disc,
a(b,s)=i A/2 Θ(b-R)

$$\sigma_{\rm el} = \pi R^2 A^2,$$
$$\sigma_{\rm tot} = 2\pi R^2 A,$$
$$\frac{\sigma_{\rm el}}{\sigma_{\rm tot}} = \frac{\Sigma_{\rm el}}{\sigma_{\rm tot}} = \frac{A}{2},$$
$$B = \frac{R^2}{4}.$$

$$\frac{d\sigma_{\rm el}}{dt} = \pi R^4 A^2 \left[\frac{J_1(qR)}{qR}\right]^2,$$

For a Gray Gaussian:
a(b,s) = i A/2 exp(-2(b/R)**2)

$$\sigma_{\rm el} = \pi R^2 A^2,$$
$$\sigma_{\rm tot} = 2\pi R^2 A,$$
$$\frac{\sigma_{\rm el}}{\sigma_{\rm tot}} = \frac{\Sigma_{\rm el}}{\sigma_{\rm tot}} = \frac{A}{2},$$
$$B = \frac{R^2}{4}.$$

$$\pi R^4 A^2 \exp[-(qR)^2/4] = \left(\frac{d\sigma_{\rm el}}{dt}\right)_{t=0} e^{-B|t|},$$

Gray Gaussian A(b) → Exponential dσ/dt.
Non-exponential dσ/dt → **a non-Gaussian behaviour** of A(b) shadow profile function

For a black disc or Gaussian, A = 1 and σ_{el}/σ_{tot} = ½ in both cases

Possible theory interpretations

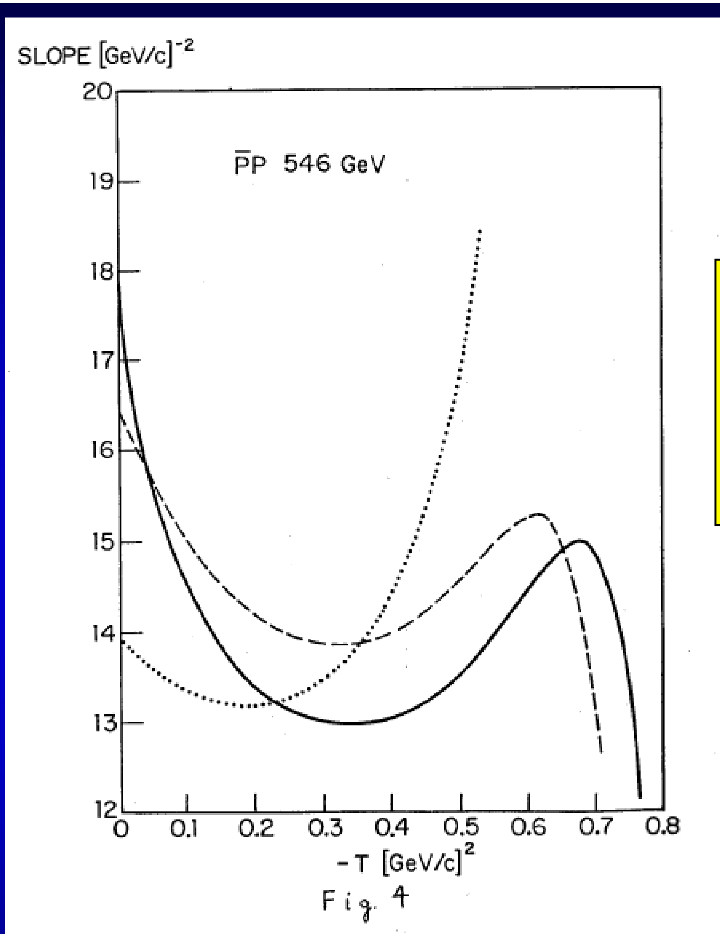

from Glauber-Velasco
PLB 147 (1984) 380
Slope is not quite
Exponential:
a non-Gaussian behaviour

ReBB: Quark-Diquark Model
Non-exponential dσ/dt:
a non-Gaussian A(b)
F. Nemes, T.Cs, M. Csanád
Int.J.Mod.Phys. A30 (2015) no.14, 1550076

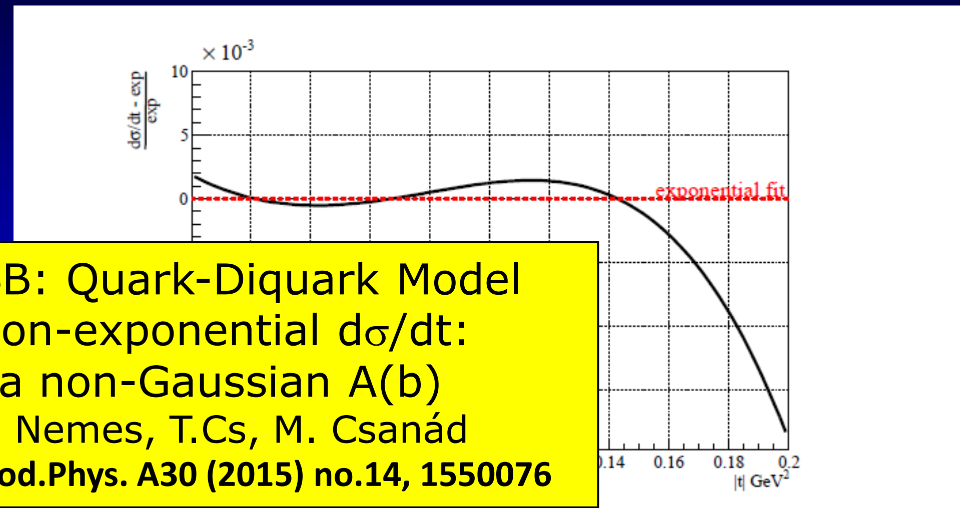

Fig. 5. The ReBB model, fitted in the $0.0 \leq |t| \leq 0.36$ GeV^2 range, with respect to the exponential fit of Eq. (33). In the plot only the $0.0 \leq |t| \leq 0.2$ GeV^2 range is shown. The curve indicates a significant deviation from the simple exponential at low $|t|$ values.

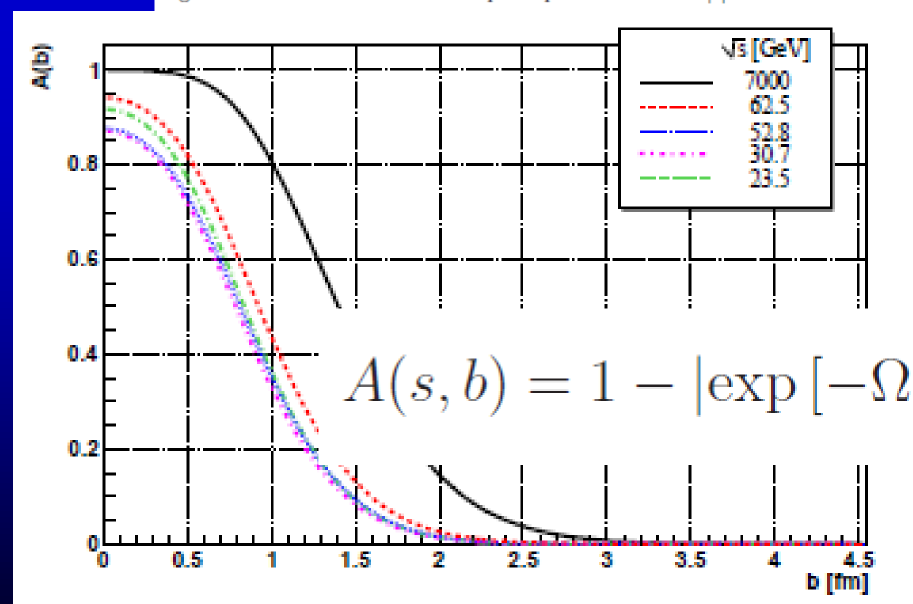

$$A(s,b) = 1 - |\exp\left[-\Omega(s,b)\right]|^2$$

Datasets on pp and ppbar, before 2015

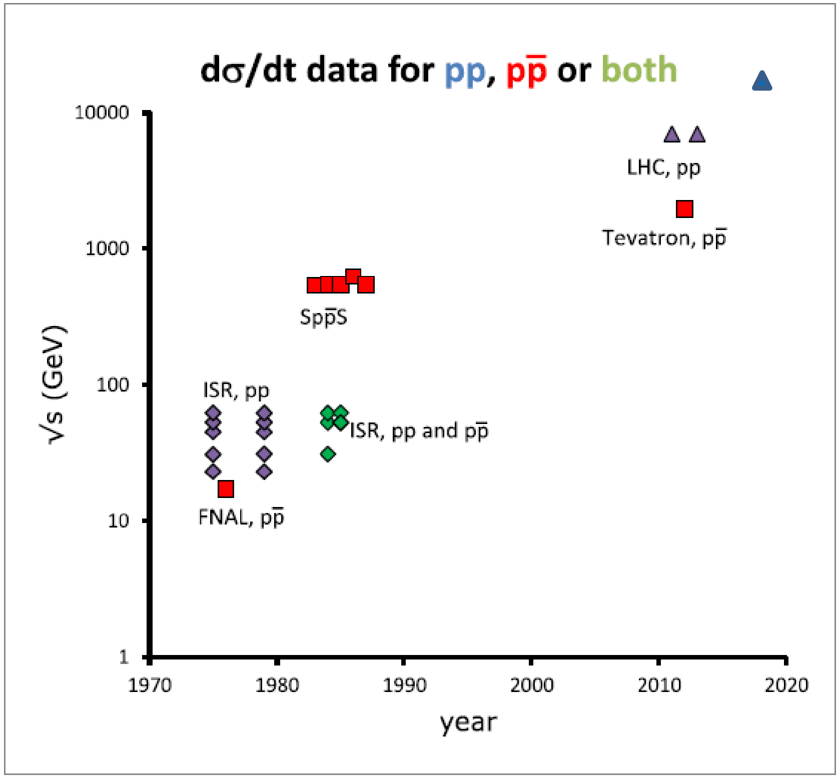

FIG. 1. Timeline of proton and antiproton elastic scattering measurements. New accelerators are run first at the maximum available energies; however, at the start of the Sp$\bar{p}$S accelerator, the pp and the $p\bar{p}$ elastic scattering data were measured at the same $\sqrt{s} = 31$, 53 and 62 GeV.

Suggests to run down LHC to ~ Tevatron energies
A. Ster, L. Jenkovszky and T. Cs, PRD 91 (2015) 074018

FNAL E-0069: evidence for non-expon

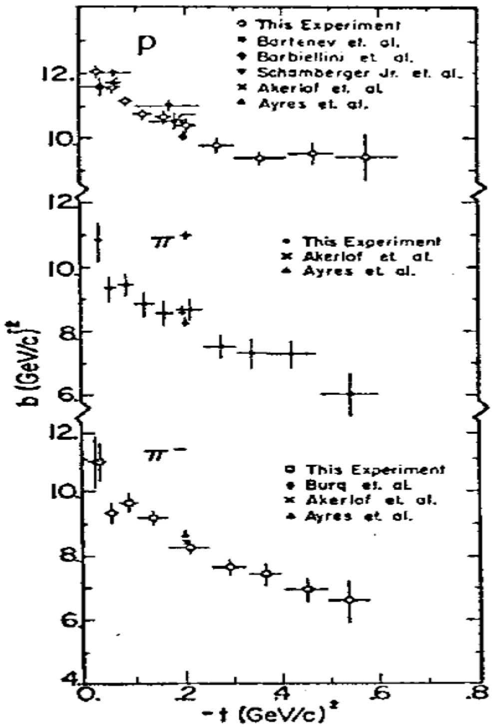

Comparison of measurements by several experiments of the logarithmic slope for $\pi^- p$, $\pi^+ p$, and pp elastic scattering.

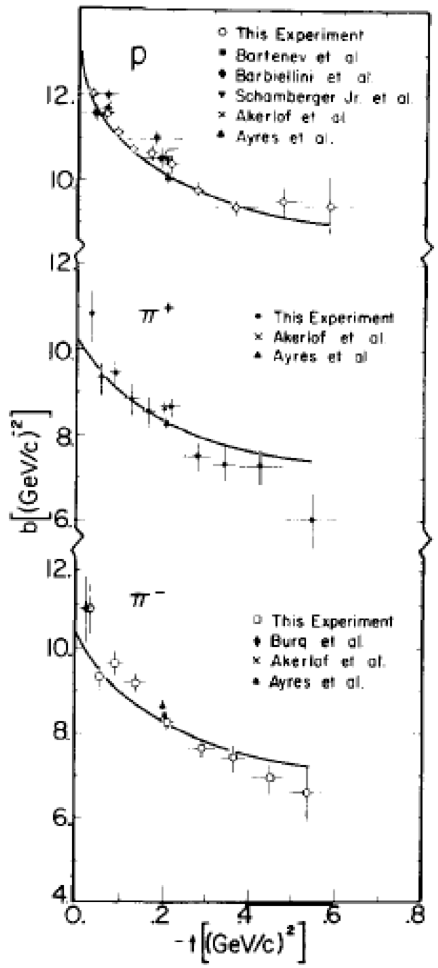

Fig. 12. Elastic slope parameters versus t at 200 GeV/c for pp, π^+p and π^-p scattering (data from ref. [14]). The curves were calculated using eq. (38), as described in the text.

[14] A. Schiz et al., Phys. Rev. D24 (1981) 26.

FNAL E-0069, A.Schiz et al.: Phys. Rev. D24 (1981) 26
Reviewed in K. Goulianos, Phys. Rept. 101 (1983) 169-219
Satisfactory fits with exp(-B(t) |t|): non-exponential in **1981**!

A. Breakstone et al. Nucl. Phys. B 248, 253 (1984).

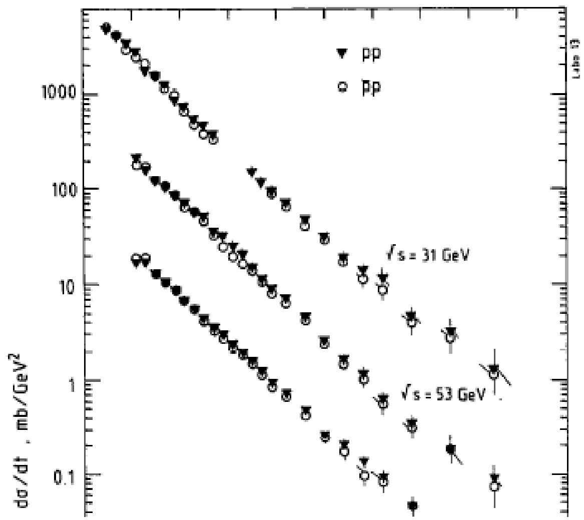

TABLE 2

Results of the fits of linear (a) and quadratic (b) exponential functions to the data

(a)

		pp			p̄p		
$\sqrt{s}$ (GeV)	$-t$ (GeV^2)	a (mb/GeV^2)	b (GeV^{-2})	χ^2/DF	a (mb/GeV^2)	b (GeV^{-2})	χ^2/DF
31	0.05–0.15	93.0 ± 5.5	11.70 ± 0.62	9.3/4	90.4 ± 5.1	11.37 ± 0.60	4.8/4
	0.17–0.85	74.0 ± 3.6	10.92 ± 0.15	12.0/16	75.6 ± 4.6	11.16 ± 0.20	14.3/14
53	0.17–0.85	72.5 ± 2.2	11.06 ± 0.11	11.9/19	78.0 ± 3.2	11.50 ± 0.15	12.0/19
62	0.17–0.85	66.4 ± 1.7	10.71 ± 0.08	11.2/9	72.3 ± 3.0	11.12 ± 0.15	9.2/19

(b)

		pp				p̄p			
$\sqrt{s}$ (GeV)	$-t$ (GeV^2)	A (mb/GeV^2)	B (GeV^{-2})	C (GeV^{-4})	χ^2/DF	A (mb/GeV^2)	B (GeV^{-2})	C (GeV^{-4})	χ^2/DF
31	0.05–0.85	99.4 ± 4.1	12.83 ± 0.34	2.64 ± 0.56	16.8/21	101.6 ± 4.0	13.06 ± 0.39	2.58 ± 0.65	17.0/19
53	0.11–0.85	62.0 ± 3.7	10.09 ± 0.47	-1.31 ± 0.74	21.8/21	70.0 ± 3.8	10.96 ± 0.44	-0.56 ± 0.74	20.5/21
62	0.11–0.85	59.9 ± 2.7	10.12 ± 2.9	-0.74 ± 0.40	28.6/21	73.4 ± 4.8	11.30 ± 0.45	0.38 ± 0.69	18.0/21

Hints non-exponential/"break":
pp@ISR, $\sqrt{s}$=21.5-52.8 GeV,
change of slope, B=B(t,s)
$|t| \sim 0.1$ GeV^2
Barbiellini et al,
Phys. Lett. B **39**, 663 (1972):
$B(t_{low}) \neq B(t_{higher})$
At $\sqrt{s}$=52.8 GeV SpbarpS
slope is same and breaks the
same way in pbarp and in pp
M. Ambrosio *et al.*
Phys. Lett. B **115**, 495 (1982).
Same slope in pp and pbar-p at
$|t| \sim 0.14$ GeV^2 ,
fits with $\exp(-B|t| - C t^2)$
at $\sqrt{s}$=31, 55, 62 GeV
A. Breakstone *et al.* Nucl. Phys. B **248**,
253 (1984).

TOTEM results at LHC before 2015

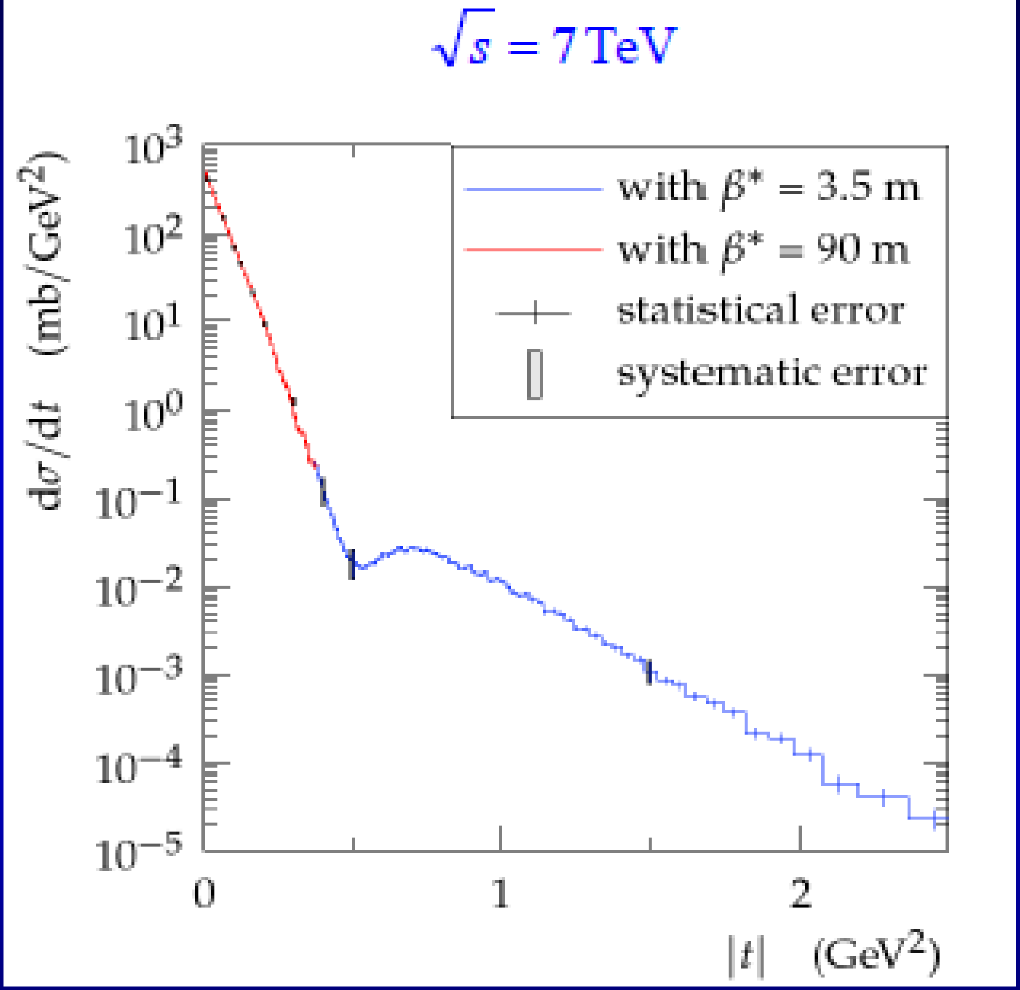

LHC data, pre-2014-15: satisfactory fits with exp(-B |t|) at low t.
TOTEM data at 8 TeV, low |t|: evidence for non-exponential cone

TOTEM: LHC Optics for Elastic pp

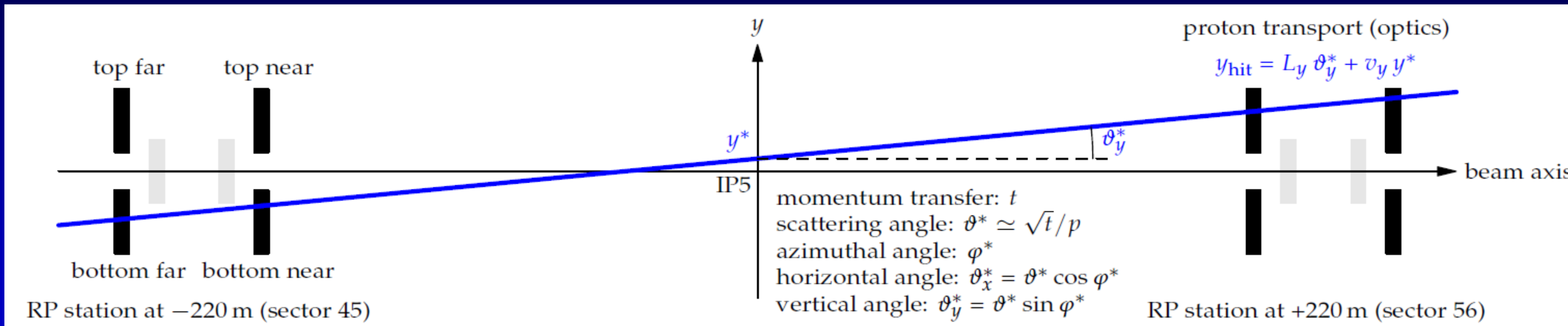

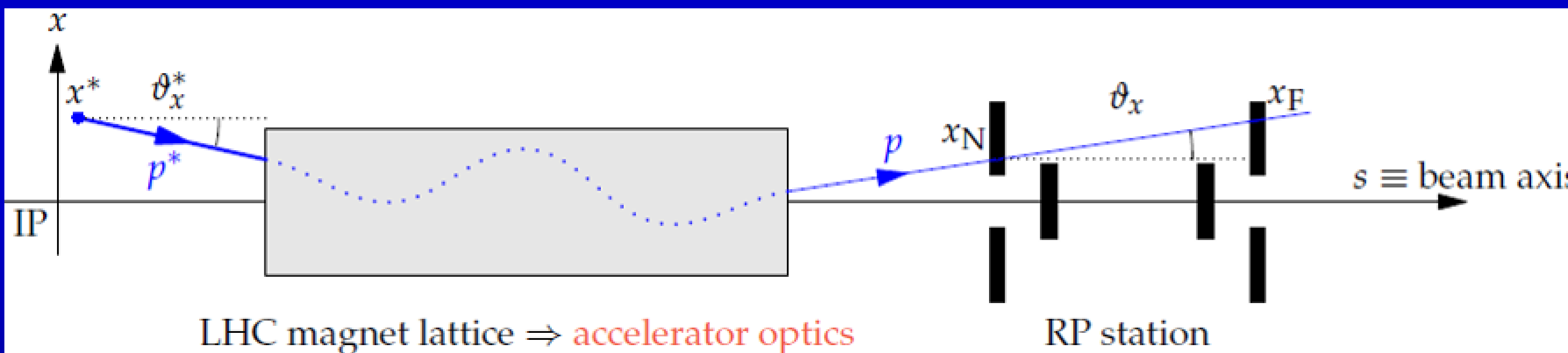

$$\begin{pmatrix} x \\ \Theta_x \\ y \\ \Theta_y \\ \Delta p/p \end{pmatrix} = \begin{pmatrix} v_x & L_x & 0 & 0 & D_x \\ v'_x & L'_x & 0 & 0 & D'_x \\ 0 & 0 & v_y & L_y & 0 \\ 0 & 0 & v'_y & L'_y & 0 \\ 0 & 0 & 0 & 0 & 1 \end{pmatrix} \begin{pmatrix} x^* \\ \Theta_x^* \\ y^* \\ \Theta_y^* \\ \Delta p/p \end{pmatrix}$$

Precise σ_{tot} and $d\sigma/dt$ determination by TOTEM needs excellent controll of LHC optics from data

LHC Optics Determination, β*= 90 m

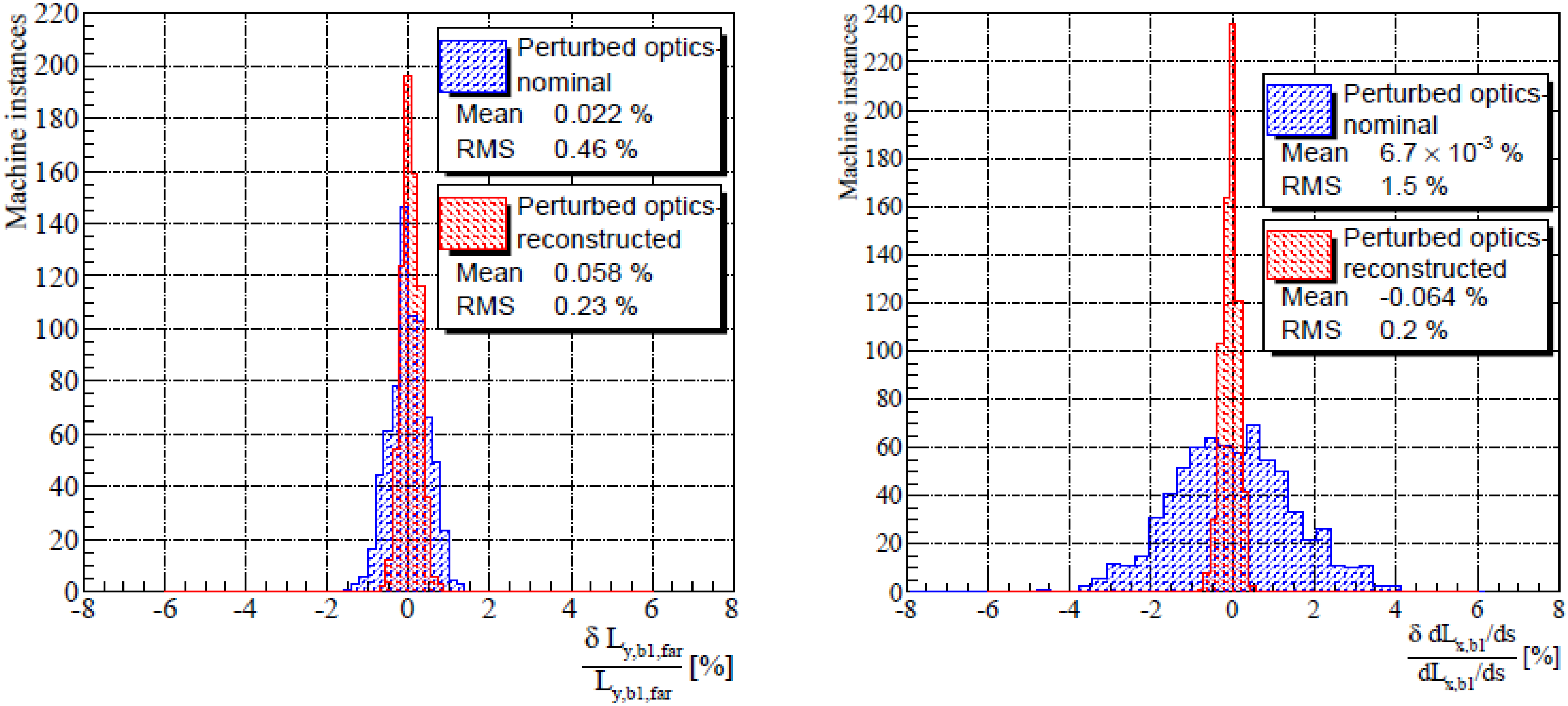

Figure 12. (color online) The MC error distribution of $\beta^* = 90$ m optical functions L_y and $\mathrm{d}L_x/\mathrm{ds}$ for Beam 1 at $E = 4$ TeV, before and after optics estimation.

TOTEM: Precise control of LHC imperfections with perturbed LHC optics and recalibration from data at IP5: factors of 2 - 10
arXiv:1406.0546

TOTEM $d\sigma/dt$ @ 8 TeV

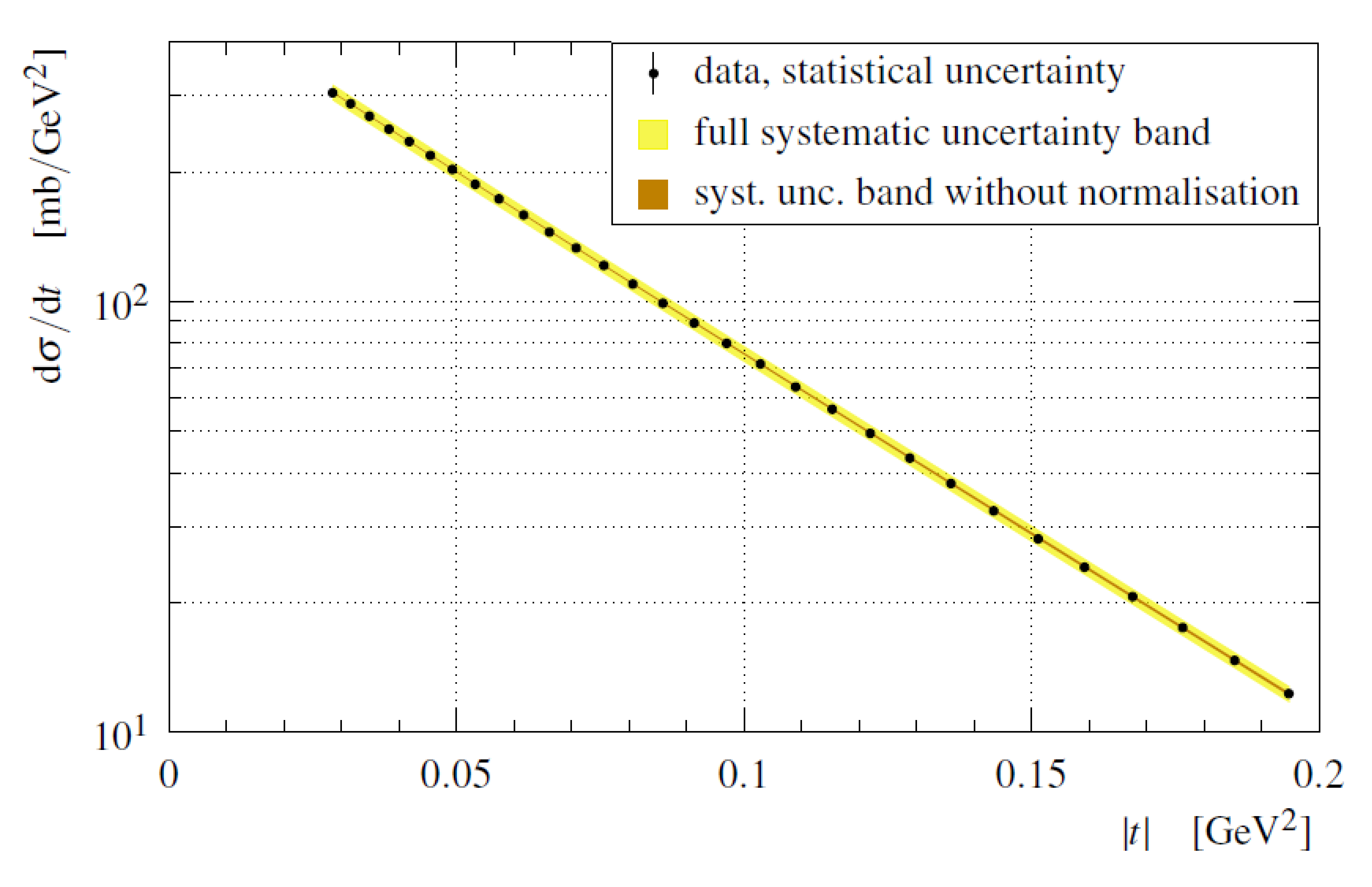

$t = -p^2\, \theta_*^2$; „optimized binning"; almost exponential but if one looks in detail, NOT

Differential cross-section @ 8 TeV

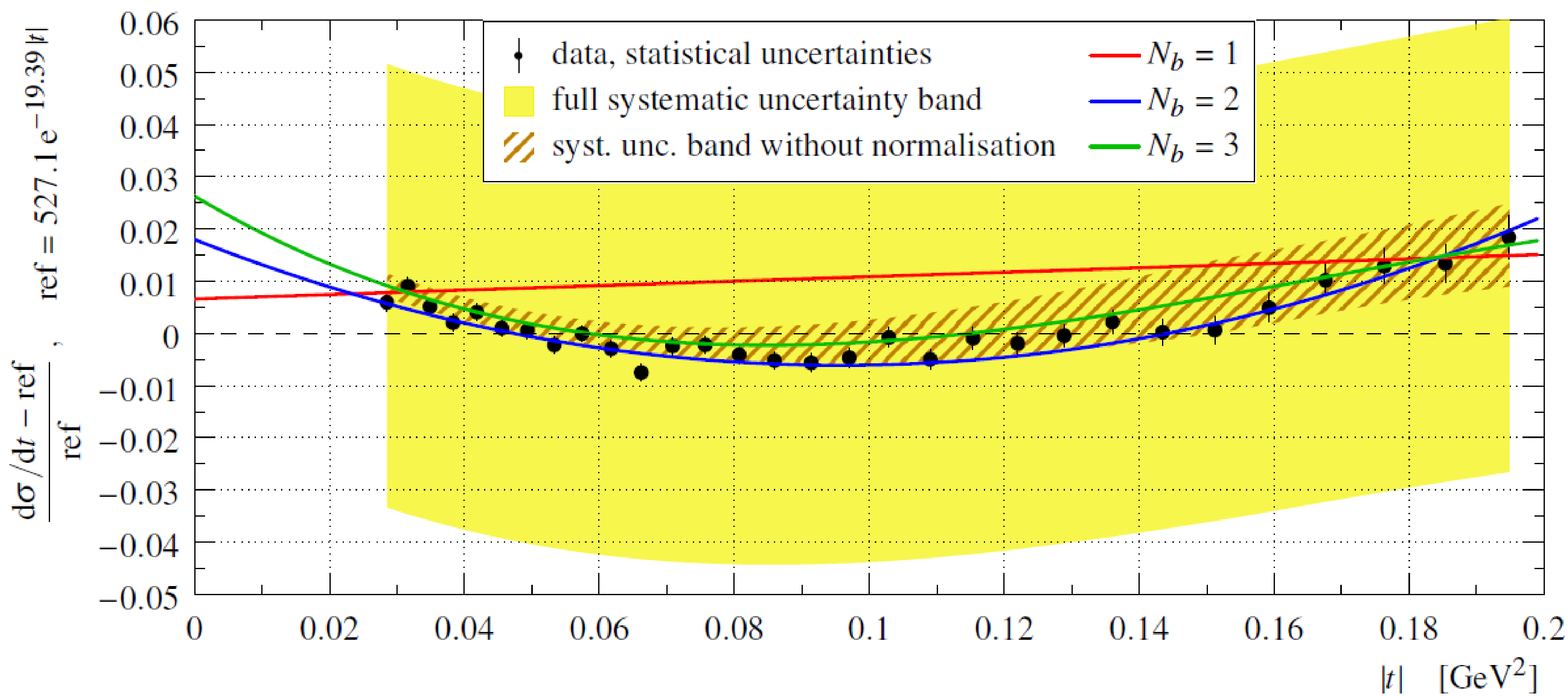

$$\frac{d\sigma}{dt}(t) = \left.\frac{d\sigma}{dt}\right|_{t=0} \exp\left(\sum_{i=1}^{N_b} b_i\, t^i\right),$$

$$\chi^2 = \Delta^T V^{-1} \Delta\,,$$

$$V = V_{stat} + V_{syst}$$

$$\Delta_i = \left.\frac{d\sigma}{dt}\right|_{\text{bin } i} - \frac{1}{\Delta t_i}\int_{\text{bin } i} f(t)\, dt\,,$$

N_b = 1 fits excluded. Relative to best exponential, a significant 7.2σ deviation found.

Differential cross-section @ 8 TeV

Table 4: Details of the fits in Figure 11 using parametrisation Eq. (15). The matrices give the correlation factors between the fit parameters.

N_b	$d\sigma/dt\vert_{t=0}$ [mb/GeV^2]	b_1 [GeV^{-2}]	b_2 [GeV^{-4}]	b_3 [GeV^{-6}]	χ^2/ndf	p-value	significance
1	531 ± 22	-19.35 ± 0.06	-	-	$117.5/28 = 4.20$	$6.2 \cdot 10^{-13}$	$7.20\,\sigma$
	$\begin{pmatrix} +1.00 & -0.11 \\ -0.11 & +1.00 \end{pmatrix}$						
2	537 ± 22	-19.89 ± 0.08	2.61 ± 0.30	-	$29.3/27 = 1.09$	0.35	$0.94\,\sigma$
	$\begin{pmatrix} +1.00 & +0.19 & -0.34 \\ +0.19 & +1.00 & -0.76 \\ -0.34 & -0.76 & +1.00 \end{pmatrix}$						
3	541 ± 22	-20.14 ± 0.15	5.95 ± 1.75	-12.0 ± 6.2	$25.5/26 = 0.98$	0.49	$0.69\,\sigma$
	$\begin{pmatrix} +1.00 & +0.08 & -0.04 & -0.02 \\ +0.08 & +1.00 & -0.90 & +0.85 \\ -0.04 & -0.90 & +1.00 & -0.99 \\ -0.02 & +0.85 & -0.99 & +1.00 \end{pmatrix}$						

$$\frac{d\sigma}{dt}(t) = \frac{d\sigma}{dt}\bigg|_{t=0} \exp\left(\sum_{i=1}^{N_b} b_i t^i\right),$$

$$\chi^2 = \Delta^T V^{-1} \Delta\,,$$

$$V = V_{stat} + V_{syst}$$

$$\Delta_i = \frac{d\sigma}{dt}\bigg|_{\text{bin } i} - \frac{1}{\Delta t_i}\int_{\text{bin } i} f(t)\,dt\,,$$

N_b = 1 fits excluded. Relative to best exponential, a significant 7.2σ deviation found.

Cross-check: „per-mille” binnings

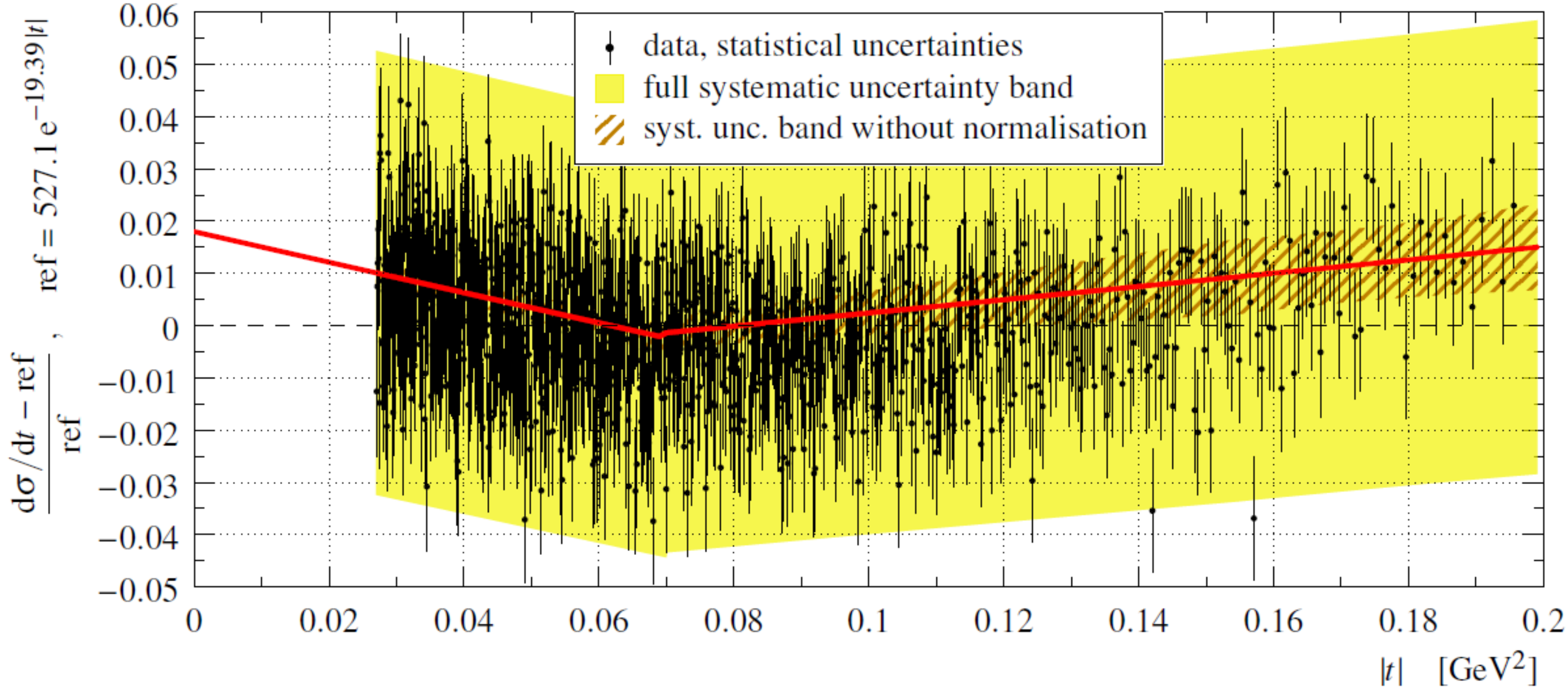

Figure 12: Differential cross-section using the "per-mille" binning and plotted as relative difference from the reference exponential (see vertical axis). The black dots represent data points with statistical uncertainty bars. The red line shows pure exponential fits in regions below and above $|t| = 0.07\,\text{GeV}^2$, see Eq. (19). The yellow band corresponds to the full systematic uncertainty, the brown-hatched one includes all systematic contributions except the normalisation. Both bands are centred around the fit curve.

$$\frac{d\sigma}{dt}(t) = \begin{cases} a_1\, e^{b_1|t|} & |t| < 0.07\,\text{GeV}^2 \\ a_2\, e^{b_2|t|} & |t| > 0.07\,\text{GeV}^2 \end{cases}$$

$$\chi_p^2 = \Delta_p^T V_p^{-1} \Delta_p\,, \quad \Delta_p = \begin{pmatrix} a_1 - a_2 \\ b_1 - b_2 \end{pmatrix}$$

Simple exp fits excluded. Different binnings show the same effect. Here 7.8 σ significance.

TOTEM dσ/dt @ 13 TeV

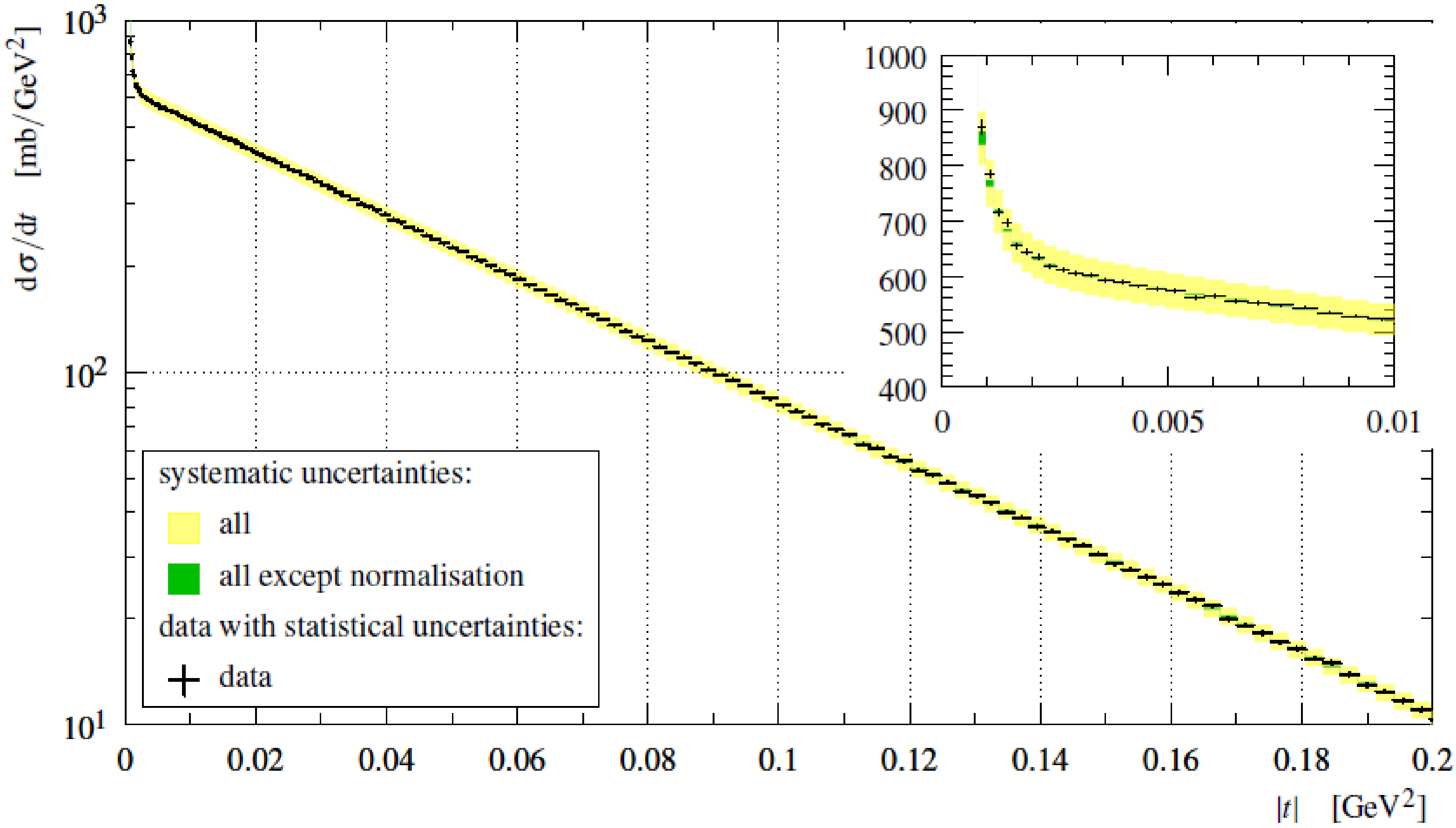

Fig. 10: Differential cross-section from Table 3 with statistical (bars) and systematic uncertainties (bands). The yellow band represents all systematic uncertainties, the green one all but normalisation. The bands are centred around a data fit including both nuclear and Coulomb components (the fit shown in Figure 14). INSET: a low-$|t|$ zoom of cross-section rise due to the Coulomb interaction.

TOTEM data from preprint CERN-PH 2017/335. Non-exponential at 13 TeV, too.

TOTEM dσ/dt @ 13 TeV, CERN-PH 2017/335

Table 5: Summary of results for various fit configurations, using the "coarse" binning.

	$\lvert t\rvert_{\max} = 0.07\,\mathrm{GeV}^2$		$\lvert t\rvert_{\max} = 0.15\,\mathrm{GeV}^2$	
N_b	χ^2/ndf	ρ	χ^2/ndf	ρ
1	0.7	0.09 ± 0.01	2.6	-
2	0.6	0.10 ± 0.01	1.0	0.09 ± 0.01
3	0.6	0.09 ± 0.01	0.9	0.10 ± 0.01

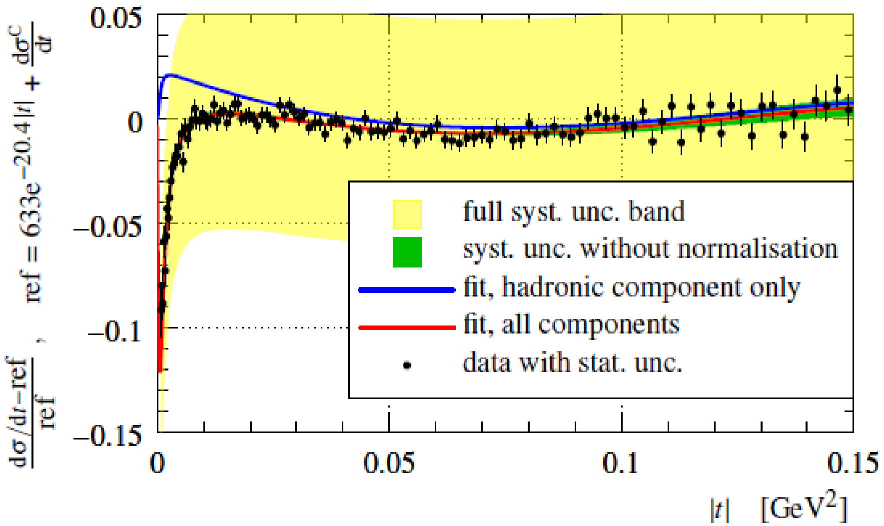

Fig. 14: Details of fit with $N_b = 3$ and $|t|_{\max} = 0.15\,\mathrm{GeV}^2$.

$$\left|\mathcal{A}^{\mathrm{N}}(t)\right| = \sqrt{\frac{s}{\pi}\frac{p}{\hbar c}\sqrt{a}\exp\left(\frac{1}{2}\sum_{n=1}^{N_b} b_n t^n\right)}$$

TOTEM: non-exponential behavior is seen clearly also at 13 TeV, but emphasis on ρ

Interpretations

TOTEM results on non-exponential behavior and indications of Odderon: triggered theoretical interpretations.

60+ theory models so far

Work in progress on reviewing these models trying to find the common, important part if possible model-independently

Only a few of all the possible models will be highlighted or summarized here

BEL or BnotEL effect?

Selyugin, arXiv:1505.02426

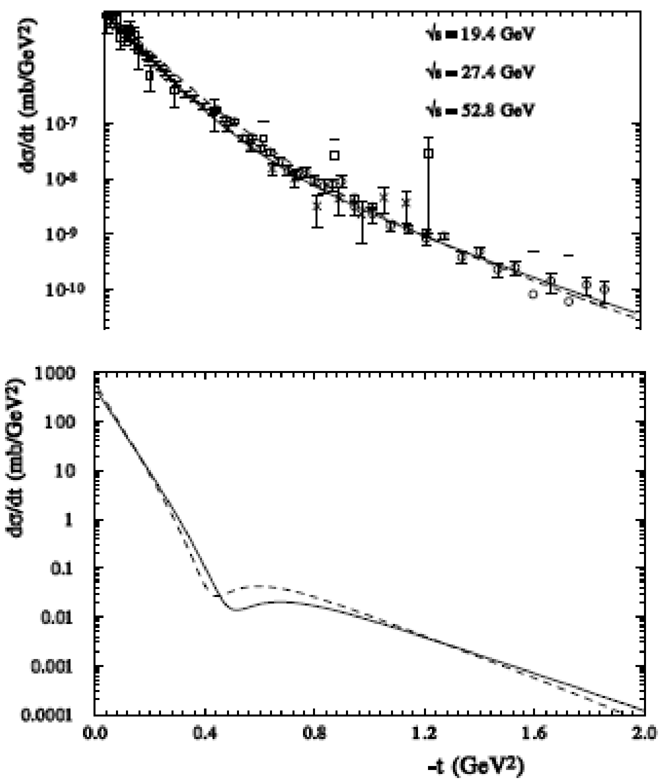

FIG. 10: The model predictions of $d\sigma/dt$ at $\sqrt{s} = 7$ (hard line) and $\sqrt{s} = 14$ TeV (dashed line).

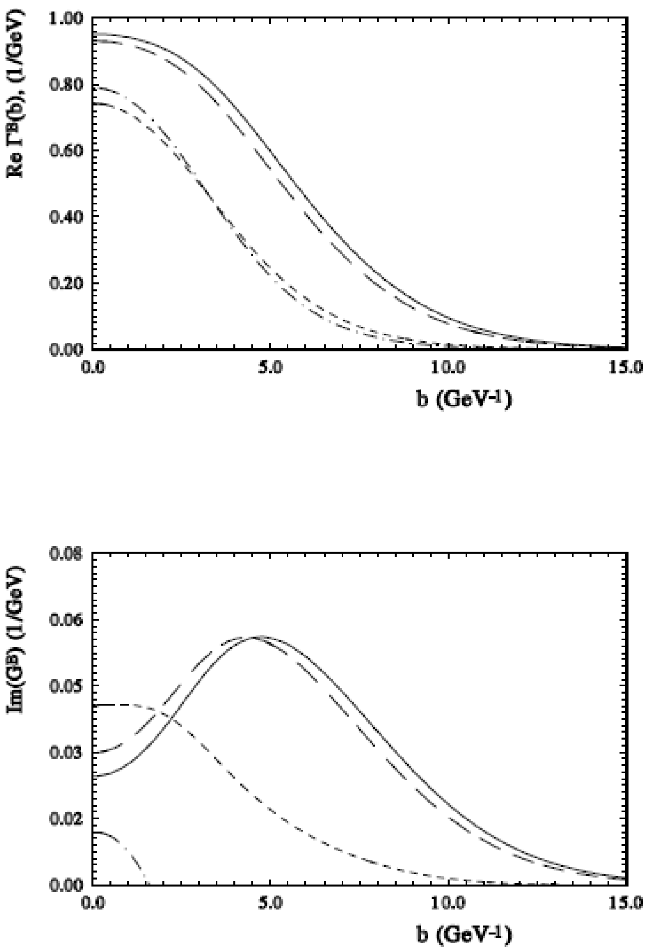

FIG. 16: The overlapping function $\Gamma(s,b)$ [for the real (top) and imaginary (bottom) parts] at $\sqrt{s} = 9.8$ GeV (dashed line), $\sqrt{s} = 52.8$ GeV (dash-dotted line), $\sqrt{s} = 7$ TeV (long dashed line), $\sqrt{s} = 14$ TeV (hard line).

Prediction:
Black disc limit is reached at LHC,
but 7 TeV data not yet fitted

Bloch, Durand, Ha, Halzen , arXiv:1505.02426

Conclusions:
The fitted data satisfy the
black disc limit within errors
but the new TOTEM data at
13 TeV data challenges
this interpretation

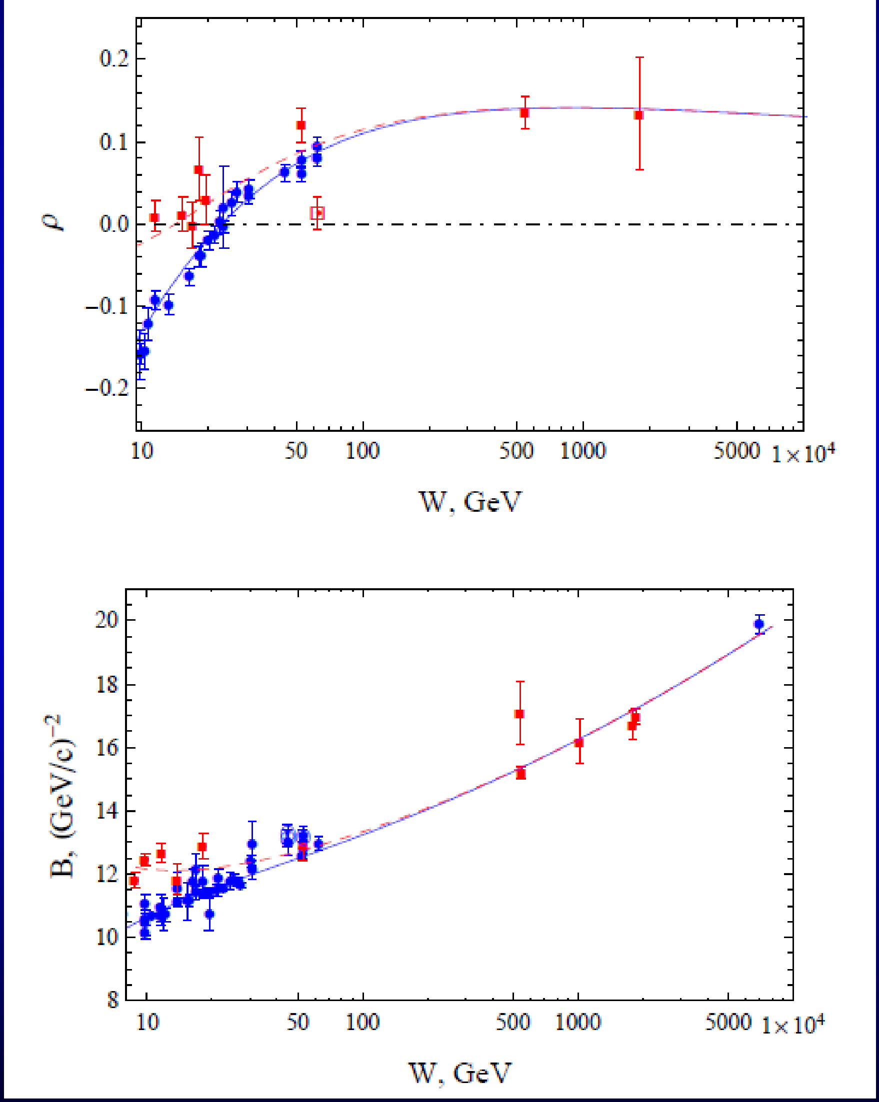

Summary

Nucl. Phys. B899 (2015) 297 by TOTEM:
low-|t| $d\sigma/dt$ for elastic pp at $\sqrt{s}$ = 8 TeV
with unprecedented precision

Significantly non-exponential behaviour
first at FNAL-0069 already,
TOTEM confirmed at 13 TeV

Theoretical interpretations:
Work in progress on reviewing them

Common picture:
Non-Gaussian shadow profile of protons
Opening of a new channel likely
Between 2.76 and 7 TeV,
New trends seen also at 13 TeV

Thank you for your attention

Questions and Comments ?

Backup slides – Questions?

LHC optics and proton acceptance

$t = -p^2\,\theta_*^2$: four-momentum transfer squared; $\xi = \Delta p/p$: fractional momentum loss

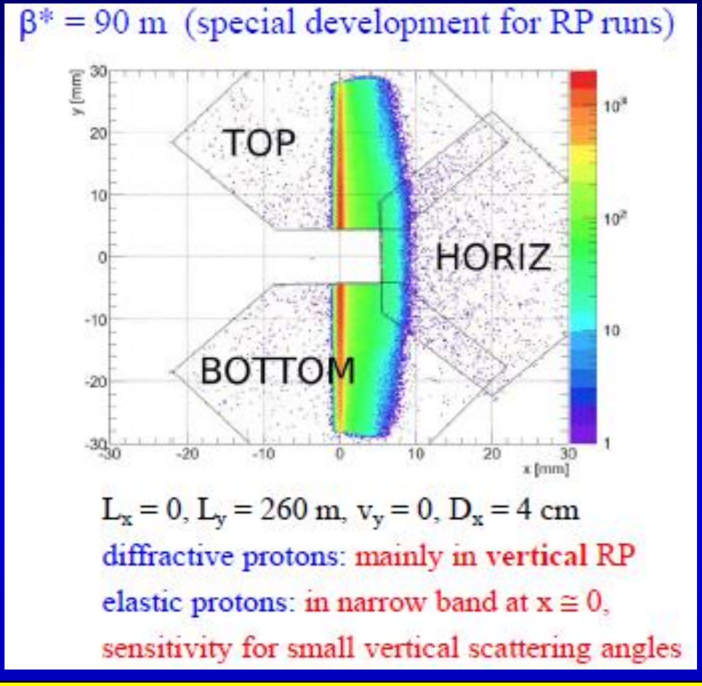

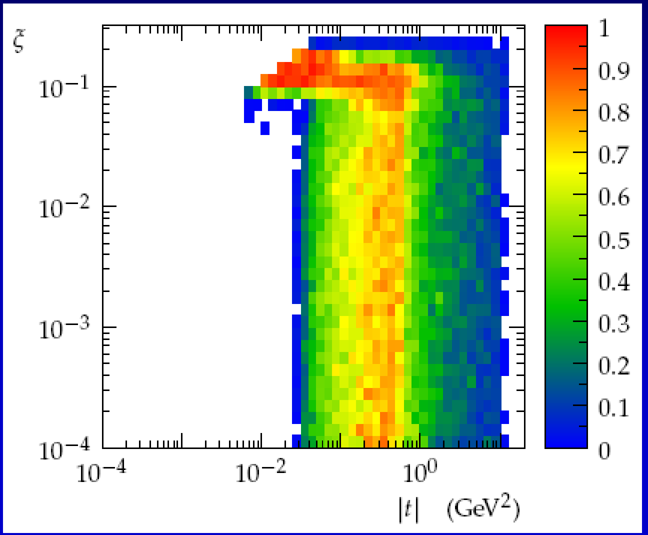

$\beta^* = 90$ m MC simulation shown
Parallel to point focussing, $v_y \sim 0$
Large effective lenght L_y
Elastic scattering events: in vertical RPs

$\beta^* = 90$ m
Diffraction:
all ξ if $|t| \geq 10^{-2}$ GeV^2,
soft & semi-hard diffr.
Elastic: low to mid $|t|$
Total cross-section

RP unit	L_x	v_x	L_y	v_y
near	2.45 m	−2.17	239 m	0.040
far	−0.37 m	−1.87	264 m	0.021

Kinematic cuts: selection of elastics

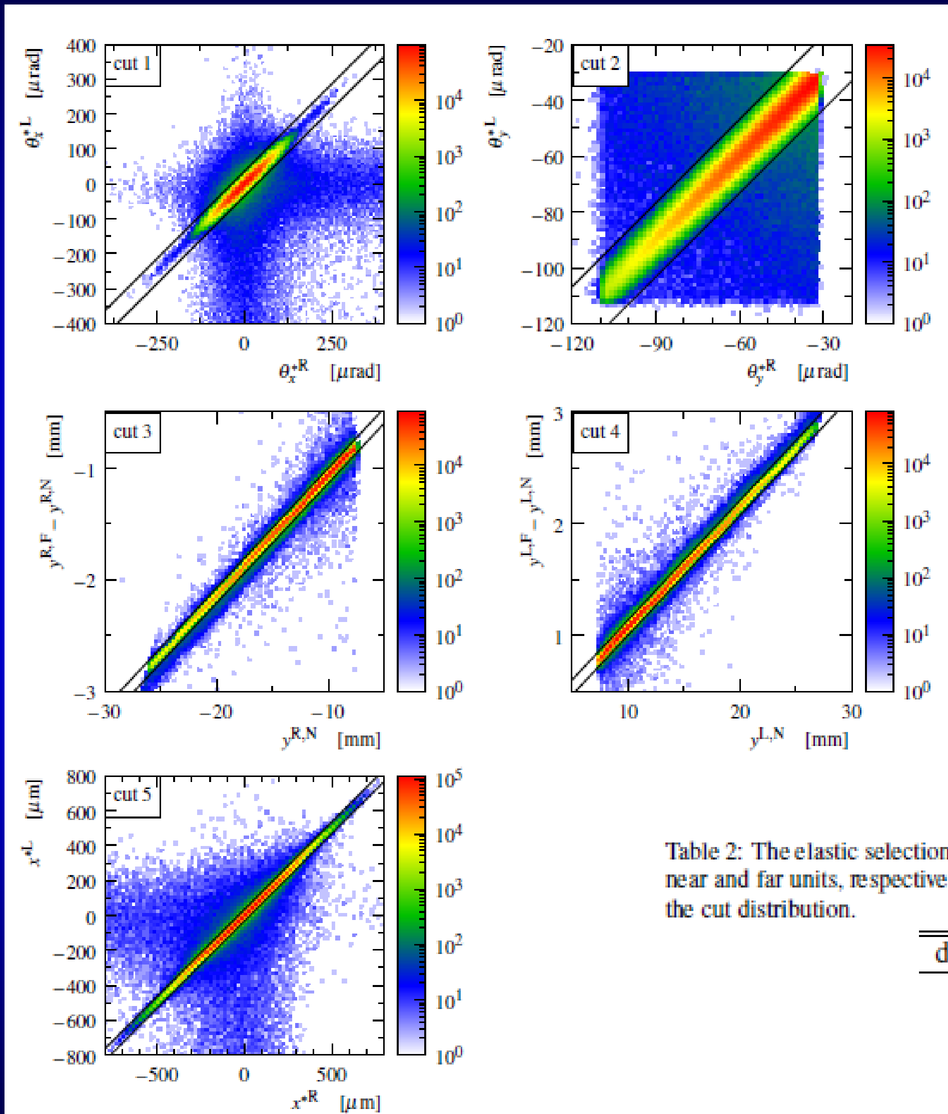

Precise control of LHC optics and elastic scattering:
Kinematics reconstruction
Alignment
Optics recalibration
Resolution unfolding
Acceptance correction
Background substraction
Detection & efficiency
Angular resolution
Normalization
Binning

Table 2: The elastic selection cuts. The superscripts R and L refer to the right and left arm, N and F correspond to the near and far units, respectively. The constant $\alpha = L_y^F / L_y^N - 1 \approx 0.11$. The right-most column gives a typical RMS of the cut distribution.

discriminator	cut quantity	RMS ($\equiv 1\sigma$)
1	$\theta_x^{*R} - \theta_x^{*L}$	9.5 μrad
2	$\theta_y^{*R} - \theta_y^{*L}$	3.3 μrad
3	$\alpha\, y^{R,N} - (y^{R,F} - y^{R,N})$	18 μm
4	$\alpha\, y^{L,N} - (y^{L,F} - y^{L,N})$	18 μm
5	$x^{*R} - x^{*L}$	8.5 μm

Backup slide – covariance matrix

Table 3: The elastic differential cross-section as determined in this analysis using the "optimised" binning. The three left-most columns describe the bins in t. The representative point gives the t value suitable for fitting [23]. The other columns are related to the differential cross-section. The four right-most columns give the leading systematic biases in $d\sigma/dt$ for 1σ-shifts in the respective quantities, δs_q, see Eqs. (13) and (14). The two contributions due to optics correspond to the two vectors in Eq. (8).

$\lvert t\rvert$ bin [GeV^2]			$d\sigma/dt$ [mb/GeV^2]						
left edge	right edge	represent. point	value	statistical uncertainty	systematic uncertainty	normalisation $\mathcal{N}$	optics mode 1	optics mode 2	beam momentum
0.02697	0.03005	0.02850	305.09	0.527	12.85	+12.83	−0.479	−0.263	+0.257
0.03005	0.03325	0.03164	287.95	0.478	12.08	+12.06	−0.502	−0.217	+0.206
0.03325	0.03658	0.03491	269.24	0.436	11.32	+11.31	−0.491	−0.174	+0.159
0.03658	0.04005	0.03831	251.31	0.401	10.59	+10.57	−0.478	−0.135	+0.115
0.04005	0.04365	0.04184	235.15	0.371	9.874	+ 9.861	−0.465	−0.0981	+0.0750
0.04365	0.04740	0.04551	218.32	0.343	9.185	+ 9.172	−0.451	−0.0647	+0.0383
0.04740	0.05129	0.04933	202.64	0.318	8.521	+ 8.509	−0.437	−0.0343	+0.0052
0.05129	0.05534	0.05330	187.10	0.295	7.882	+ 7.870	−0.421	−0.0070	−0.0244
0.05534	0.05956	0.05743	173.06	0.274	7.270	+ 7.257	−0.405	+0.0172	−0.0504
0.05956	0.06394	0.06173	158.77	0.255	6.685	+ 6.672	−0.388	+0.0385	−0.0731
0.06394	0.06850	0.06620	144.93	0.236	6.127	+ 6.114	−0.370	+0.0569	−0.0925
0.06850	0.07324	0.07085	133.12	0.219	5.597	+ 5.584	−0.352	+0.0724	−0.109
0.07324	0.07817	0.07568	121.24	0.203	5.096	+ 5.082	−0.334	+0.0853	−0.122
0.07817	0.08329	0.08071	109.77	0.188	4.623	+ 4.609	−0.316	+0.0957	−0.132
0.08329	0.08862	0.08593	99.077	0.174	4.179	+ 4.164	−0.297	+0.104	−0.140
0.08862	0.09417	0.09137	89.126	0.161	3.762	+ 3.747	−0.279	+0.109	−0.145
0.09417	0.09994	0.09702	79.951	0.148	3.374	+ 3.359	−0.260	+0.113	−0.147
0.09994	0.10593	0.10290	71.614	0.137	3.014	+ 2.998	−0.242	+0.115	−0.148
0.10593	0.11217	0.10902	63.340	0.125	2.680	+ 2.664	−0.224	+0.115	−0.147
0.11217	0.11866	0.11538	56.218	0.115	2.373	+ 2.357	−0.206	+0.114	−0.144
0.11866	0.12540	0.12199	49.404	0.105	2.092	+ 2.075	−0.189	+0.111	−0.139
0.12540	0.13242	0.12887	43.300	0.0961	1.835	+ 1.818	−0.173	+0.107	−0.134
0.13242	0.13972	0.13602	37.790	0.0876	1.601	+ 1.585	−0.157	+0.102	−0.127
0.13972	0.14730	0.14346	32.650	0.0795	1.391	+ 1.374	−0.142	+0.0974	−0.120
0.14730	0.15520	0.15120	28.113	0.0720	1.201	+ 1.185	−0.127	+0.0924	−0.112
0.15520	0.16340	0.15925	24.155	0.0659	1.030	+ 1.016	−0.0955	+0.0866	−0.104
0.16340	0.17194	0.16761	20.645	0.0616	0.877	+ 0.866	−0.0590	+0.0804	−0.0951
0.17194	0.18082	0.17632	17.486	0.0574	0.743	+ 0.733	−0.0302	+0.0739	−0.0865
0.18082	0.19005	0.18537	14.679	0.0543	0.626	+ 0.617	−0.0081	+0.0673	−0.0780
0.19005	0.19965	0.19478	12.291	0.0504	0.524	+ 0.515	+0.0052	+0.0606	−0.0697

Backup slide: systematics

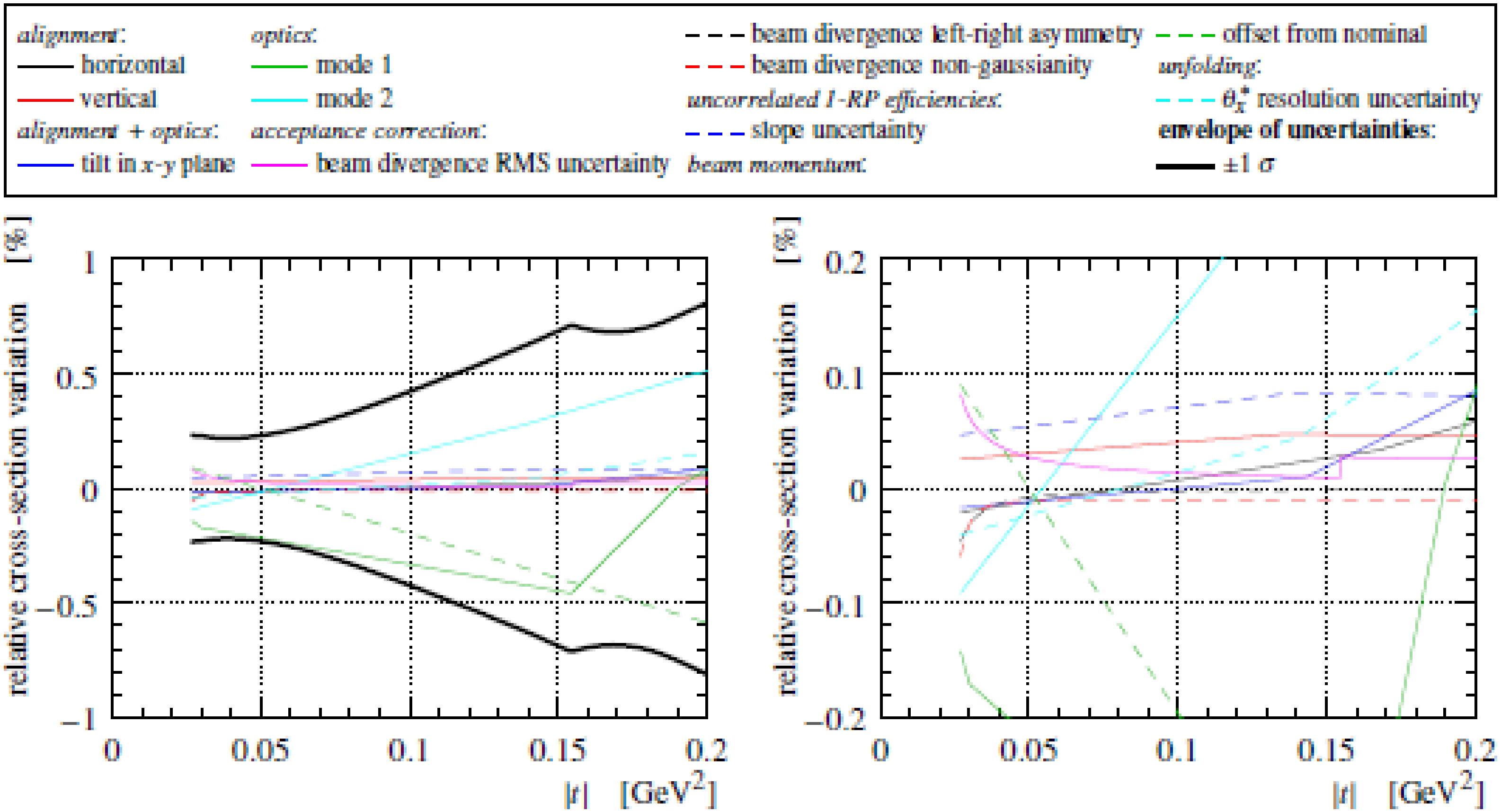

Figure 9: Impact of t-dependent systematic effects on the differential cross-section. Each curve corresponds to a systematic error at 1 σ, cf. Eq. (13). The two contributions due to optics correspond to the two vectors in Eq. (8). The envelope is determined by summing all shown contributions in quadrature for each $|t|$ value. The right-hand plot provides a vertical zoom; note that the envelope is out of scale.

No significant effect found on the total pp cross-section, σ_{tot}

TOTEM physics at LHC

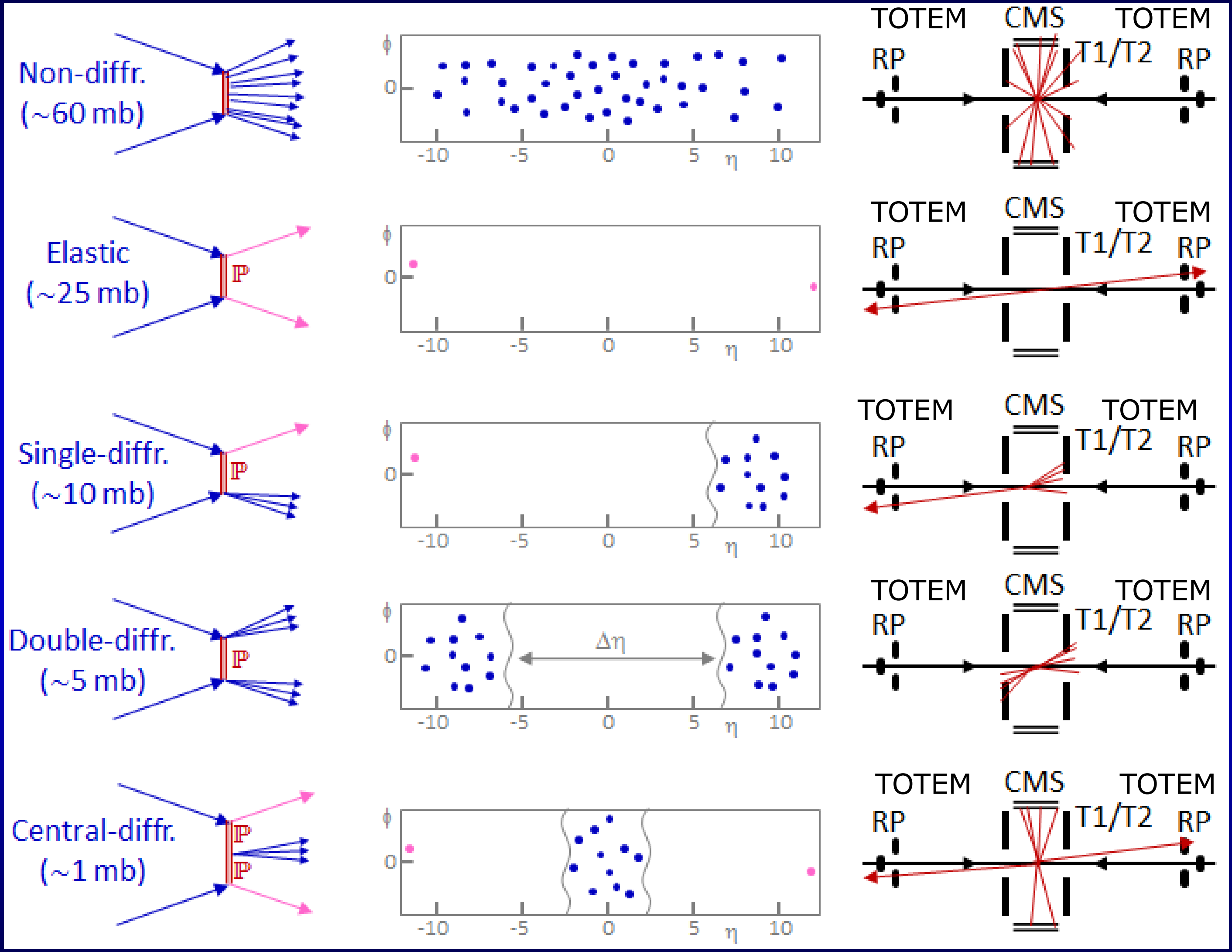

Elastic and diffractive scattering: colorless exchange